Proceedings Paper:
Na'inna, AM, Somuano-Ballesteros, HN, Phylaktou, HN et al. (1 more author) (2014) Flame Acceleration in Tube Explosions with up to Three Flat-bar Obstacles with Variable Obstacle Separation Distance. In: Proceedings. Tenth International Symposium on Hazard, Prevention and Mitigation of Industrial Explosions (X ISHPMIE), 10-14 Jun 2014, Bergen, Norway. . ISBN 978-82-999683-0-0

Na'inna, A., Phylaktou, H.N. and Andrews, G.E., Flame acceleration in tube explosions with up to three flat-bar obstacles with variable obstacle separation distance. Tenth International Symposium on Hazards, Prevention, and Mitigation of Industrial Explosions (XISHPMIE) Bergen, Norway, 10-14 June 2014

Flame Acceleration in Tube Explosions with up to Three Flat-bar Obstacles with Variable Obstacle Separation Distance

Na'inna A.M., G. Somuano-Ballesteros, H.N. Phylaktou & G.E. Andrews

E-mail: *pm08amn@leeds.ac.uk*

Energy Research Institute University of Leeds, Leeds, United Kingdom

Abstract

The effect of obstacle separation distance on the severity of gas explosions has received little methodical study. It was the aim of this work to investigate the influence of obstacle spacing of up to three flat-bar obstacles. The tests were performed using methane-air (10% by vol.), in an elongated vented cylindrical vessel 162 mm internal diameter with an overall length-to-diameter, L/D, of 27.7. The obstacles had either 2 or 4 flat-bars and presenting 20% blockage ratio to the flow path. The different number of flat-bars for the same blockage achieved a change of the obstacle scale which was also part of this investigation. The first two obstacles were kept at the established optimum spacing and only the spacing between the second and third obstacles was varied. The profiles of maximum flame speed and overpressure with separation distance were shown to agree with the cold flow turbulence profile determined in cold flows by other researchers. However, the present results showed that the maximum effect in explosions is experienced at 80 to 100 obstacle scales about 3 times further downstream than the position of maximum turbulence determined in the cold flow studies. Similar trends were observed for the flames speeds. In both cases the optimum spacing between the second and third obstacles corresponded to the same optimum spacing found for the first two obstacles demonstrating that the optimum separation distance does not change with number of obstacles. In planning the layout of new installations, the worst case separation distance needs to be avoided but incorporated when assessing the risk to existing set-ups. The results clearly demonstrate that high congestion in a given layout does not necessarily imply higher explosion severity as traditionally assumed. Less congested but optimally separated obstructions can lead to higher overpressures.

Keywords: *gas explosions, obstacles, obstacle separation, turbulence intensity*

Need nomenclature table

1. Introduction

Investigators of gas explosions in congested volumes as typically found in industrial layouts, have identified a number of important obstacle characteristics that affect the severity the explosion (in addition to the combustion chemistry). These include: blockage ratio, size, shape, scale, location of obstacles relative to the ignition and the path of flame propagaton, the number of obstacles, and spacing between the obstacles. The separation distance (pitch) between obstacles is one of the areas that has not received adequate attention by the

researchers despite general recognition of the important role it plays in determining the explosion severity. According to Lee and Moen (1980), sustained flame acceleration could not be attained for large pitch due to decay of turbulence in between obstacles while for small pitch the pocket of unburned gas between the obstacles would be too small to allow for the flame to accelerate before reaching the next obstacle. In between there has to be a worst case explosion interaction obstacle spacing and there is no previous work that determines this. In compliance with the ATEX directive (ATEX, 1994), the worst case scenarios need to be used in assessing the severity of the hazard posed by gas explosions in process plant or offshore oil and gas platforms. In planning the layout of new installations, it is appropriate to identify the relevant worst case obstacle separation in order to avoid it. In assessing the risk to existing installations and taking appropriate mitigation measures it is important to evaluate such risk on the basis of a clear understanding of the effects of separation distance and congestion.

A number of experimental explosion studies have demonstrated the effect of obstacle separation distance as part of wider assessment of the effects of congestion. These include the works of: Moen *et al.* (1980); Moen *et al.* (1982); Chan *et al.* (1983); Harrison and Eyre (1987); Lindstedt and Michels (1989); Teodorczyk *et al.* (1989); Mercx (1992); Beauvais *et al.* (1993); Obara *et al.* (1996); Mol'kov *et al.* (1997); Yu *et al.* (2002); Cicarelli *et al.* (2005); Teodorczyk *et al.* (2009); Rudy *et al.* (2011); Vollmer *et al.* (2011); Pang *et al.* (2012); Boeck *et al.* (2013) and Porowski and Teodorczyk (2013). The bulk of studies was performed with repeat obstacles spaced over a short distance, the spacing between obstacles was small and varied just from 1.3 to 10 characteristic obstacle scales. However, this is not up to the range of 3 to 20 characteristic obstacle scales downstream of the grid where the maximum combustion rate usually occurs as discussed by Phylaktou and Andrews (1991).

The authors (Na'inna *et al.,* 2013a) reported an experimental study in an elongated tube with two orifice plate obstacles of 30% blockage ratio each, where the obstacle separation distance was varied systematically from 0.5 m to 2.75 m. They reported a direct influence of the obstacle separation distance on flame speed and overpressure. A separation distance of 1.75 m produced close to 3 bar overpressure and a flame speed of about 500 m/s with 10% methane/air explosions. These values were of the order of twice the overpressure and flame speed with a separation pitch of 2.75 m. The profile of effects with separation distance was shown to agree with the turbulence profile determined in cold flows by other researchers. However, the experimental results showed that the maximum effect in explosions was experienced further downstream than the position of maximum turbulence determined in the cold flow studies. Also, the authors (Na'inna *et al.,* 2013b) investigated the influence of mixture reactivity and fuel type on the optimum obstacle separation distance for generation using two induced turbulent generating orifice plates of 30% blockage with variable obstacle spacing.

It was the aim of this work to extend the investigation into the experimental assessment of the influence of obstacle spacing using three obstacles of variable number of flat-bars (obstacle scale, b) with fixed 20% blockage ratio..

2. Experiments

A long cylindrical vessel 162 mm internal diameter made from nine flanged sections, 8 of them of 0.5 m length each and one section 0.25m in length (total nominal length of 4.25m). The test vessel was rated to withstand an overpressure of 35 bar. It was was mounted horizontally and closed at the ignition end, with its open end connected to a large cylindrical dump-vessel with a volume of 50 m^3. This arrangement enabled the simulation of open-to-

atmosphere explosions with accurate control of both test and dump vessels pre-ignition conditions.

Up to three obstacles (flat-bar types) with different number of bars as shown in Fig. 1 made from stainless steel of 3.2 mm thick, and 20% blockage were used in the test vessel. The different number of flat-bars for the same blockage achieved a variation of the obstacle scale, b (width of the bar), which was also part of this investigation.

Figure 1: Turbulence generation obstacles: two and four flat-bar obstacles of 20% blockage each.

The obstacles were mounted between the section flanges. For the double obstacle tests, the first obstacle was positioned 1 m downstream of the spark (for all tests) while the second obstacle's position was varied from 0.25 m to 2.75 m downstream of the first obstacle in order to obtain the worst case obstacle spacing. For the triple obstacle tests, the first two obstacles were kept at the established worst case spacing and only the spacing between second and third obstacles was changed.

A pneumatically actuated gate valve isolated the test vessel prior to mixture preparation. A vacuum pump was used to evacuate the test vessel before a 10 % (by vol.) methane-air mixture was formed using partial pressures, to a total mixture pressure of 1 atm. The dump vessel was filled with air to a pressure of 1 atm as well. After mixture circulation, allowing for at least 4 volume changes, the gate valve to the dump vessel was opened and a 16 Joule spark plug ignition was effected at the centre of the test vessel closed-end flange. The test vessel had an overall length-to-diameter ratio, L/D of 27.7. The set-up is shown in Fig. 2.

(a)

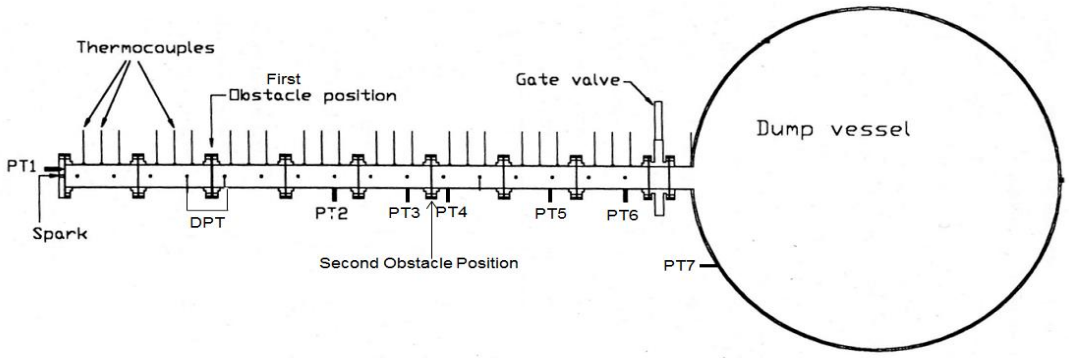

(b)

Figure 2: Experimental set-up (a) Photograph (b) Schematic diagram.

An array of 24 type-K mineral insulated exposed junction thermocouples positioned along the axial centre line of the test vessel was used to record the time of flame arrival. Average flame speeds allocated to the midway position between two thermocouples were obtained by dividing the distance between two thermocouples by the difference in time of flame arrival at each thermocouple position. A smoothing algorithm was applied to the flame arrival data, as described by Gardner (1998), to avoid either high or negative flame speeds where the flame brush appears to arrive at downstream centreline locations earlier than upstream ones, particularly in the regions of strong acceleration downstream of the obstacles.

The test vessel and dump vessel pressure histories were recorded using an array of 8 Keller-type pressure transducers - 7 gauge pressure transducers (PT1to PT7) and 1 differential (DPT), as shown in Fig. 2. Wall static pressure tapping measured by a differential pressure transducer (DPT) were located at 0.5D upstream and 1D downstream of the first obstacle as specified by BS5167-2 (2003). Pressure transducers, PT3 and PT4 were positioned 0.5D upstream and 1D downstream of the second obstacle and they were used to obtain the pressure differential across these obstacles. For the third obstacle tests, PT2 and PT5 (0.5D and 1D upstream and downstream respectively) were used to measure the pressure drop across such obstacles and these were used in calculating the induced gas flow velocities and other flow turbulence characteristics (but these are not reported in this paper). Pressure transducers PT1 and PT6 were positioned permanently at the ignition position-end flange and end of the test vessel (25D from the spark) respectively. The pressure history in the dump vessel was measured using PT7 positioned as shown in Fig.2.

A 32-channel (maximum sampling frequency of 200 KHz per channel) transient data recorder (Data Logger and FAMOS) was used to record and process the explosion data. Each test was conducted three times in order to demonstrate repeatability and ensure representative data and the average of the repeat tests was used for the analysis of the flame speed and overpressure.

Table 1 shows a list of the tests carried out as part of this work and an overview of the results.

Table 1: Summary of test conditions and results.(explain symbols)

Test	N_{obst}	N_b	b	x_{s1}	x_{s2}	x_{s1}/b	x_{s2}/b	S_{fmax}	P_{max}
(-)	(-)	(-)	(m)	(m)	(m)	(-)	(-)	(m/s)	(bar)

1	-	-	-	-	-	-	-	122	0.26
2	1	2	0.013	-	-	-	-	227	0.56
3	2	2	0.013	1	-	78	-	333	0.98
4	2	2	0.013	1.25	-	98	-	386	1.18
5	2	2	0.013	1.75	-	137	-	360	1.08
6	3	2	0.013	1.25	1	98	78	489	1.90
7*	3	2	0.013	1.25	1.25	98	98	569	2.16
8*	3	2	0.013	1.25	1.75	98	137	338	1.68
9	1	4	0.006	-	-	-	-	206	0.43
10	2	4	0.006	0.25	-	39	-	276	0.97
11	2	4	0.006	0.5	-	78	-	356	1.10
12	2	4	0.006	1	-	156	-	348	0.77
13	3	4	0.006	0.5	0.25	78	39	469	1.79
14	3	4	0.006	0.5	0.5	78	78	498	2.00
15	3	4	0.006	0.5	0.75	78	117	387	1.63
16	3	4	0.006	0.5	1.25	78	195	349	1.18

* An extra pipe section of about 0.25 m length and 0.162 m diameter was used to have equal spacing within the three obstacles

3. Results and discussion

3.1 Influence of Obstacle Spacing on Two Obstacles

Figure 3 presents the maximum overpressure and dimensionless obstacle spacing for two 4-flat-bar obstacles. Also shown is the intensity of turbulence profile against the dimensionless distance downstream of a bar-grid obstacle of 0.22 BR from Baines and Peterson (1951). It was observed that the maximum overpressure increased with the reduction in number of flat-bars. This was as a result of the increase in obstacle scale, b with decrease in number of flat-bars. A maximum overpressure of about 1.18 bar at 1.25 m obstacle spacing (98 obstacle scales) was achieved with 2-flat-bar whereas 4-flat-bar obstacles produced a maximum overpressure of 1.10 bar at 0.5 m obstacle spacing (78 obstacle scales). This shows as the obstacle scale increased the optimum obstacle spacing also increased in absolute terms. However the optimum obstacle separation distance in terms of number of obstacle scale was roughly constant between 80 and 100 within the resolution of the data due the limited spacing distances possible in the experiments.

The qualitative overall pattern of the maximum overpressure with dimensionless obstacle spacing for all the obstacles was similar to the turbulence intensity profile from Baines and Peterson (1951) see Fig.3. For nearly equal obstacle blockage ratio (0.2 BR) between the cold flow and the present work, the present results showed that the maximum effect in explosions is experienced further downstream (about 3 times the distance) than the position of maximum turbulence determined in the cold flow studies. It is suggested that this may be due to the detachment of the turbulence region from the obstacle, once the flame goes through the obstacle, and the subsequent convection of the turbulent flow plug ahead of the propagating flame, while the flame simultaneously burns into it.

The effect of maximum flame speeds on dimensionless obstacle spacing between two obstacles for 2 and 4 flat-bar obstacles is shown in Fig. 4. The general profiles of maximum flame speed and their dependence on obstacle scale and obstacle spacing were similar to those observed for the maximum overpressure results.

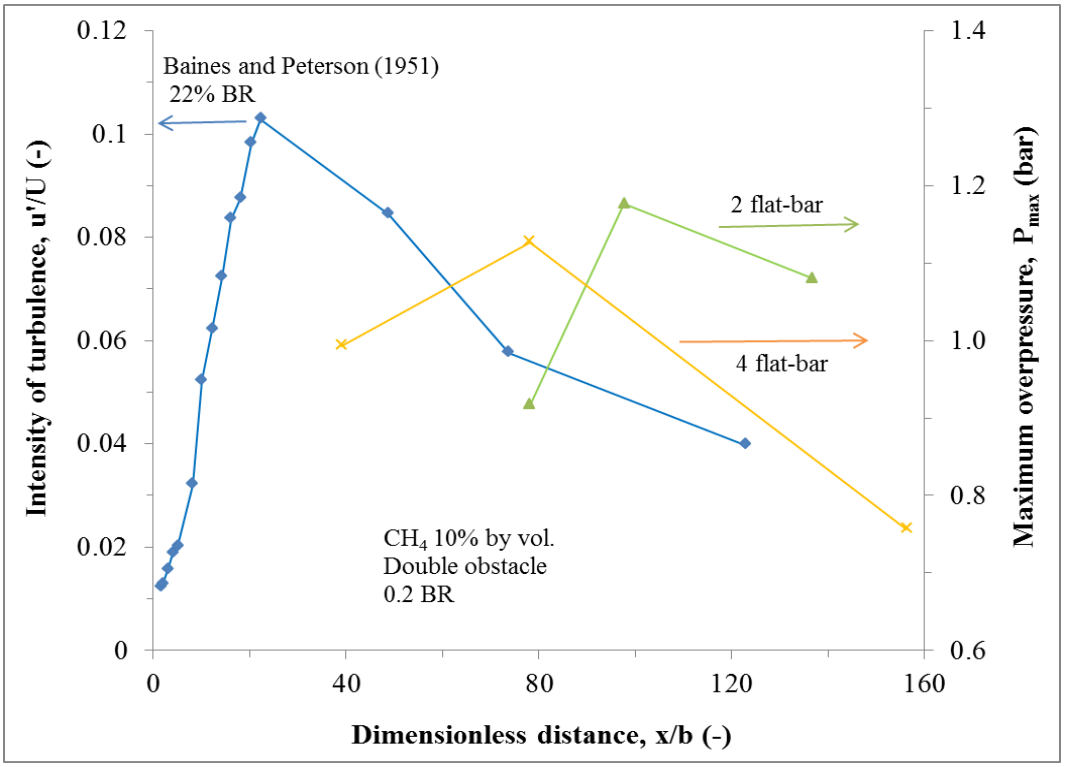

Figure 3: Comparison between intensity of turbulence from cold flow turbulence and transient experimental work with flat-bar obstacles.

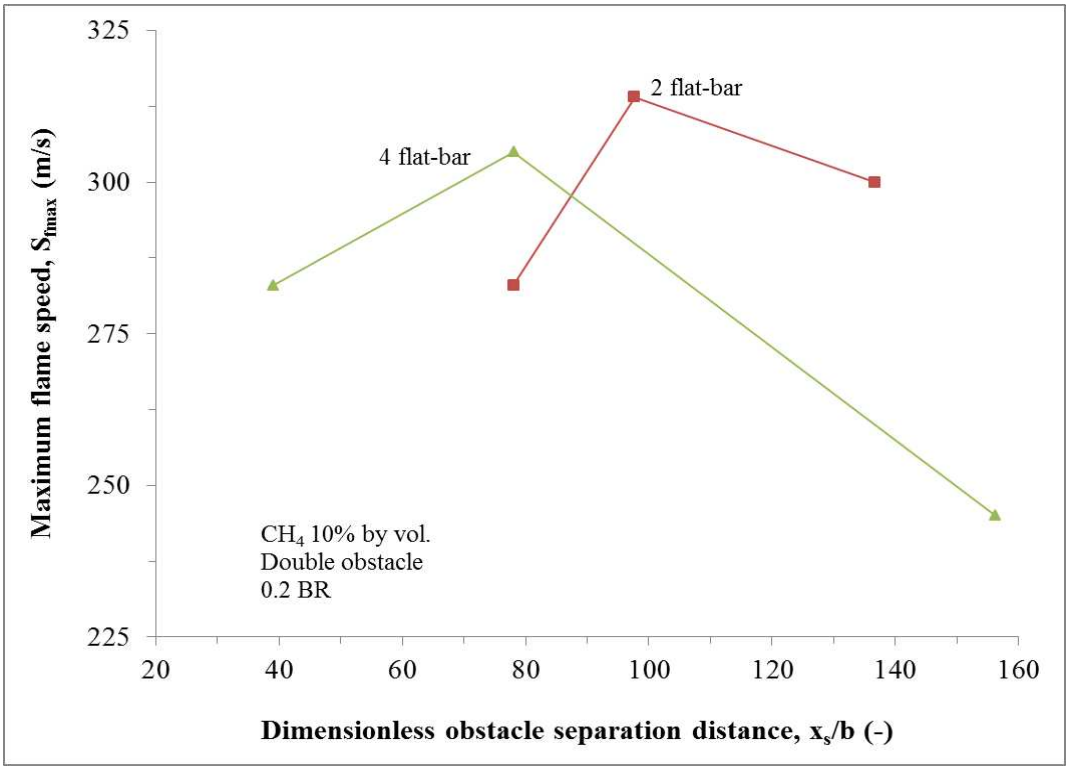

Figure 4: Influence of obstacle scale on maximum flame speeds and dimensionless obstacle spacing.

3.2 Optimum Spacing of the Third Obstacle

The positioning of the third obstacle was investigated by keeping the positioning of the first two obstacles for optimum acceleration as established in 3.1, and changing only the position of the third obstacle relative to the second . Figure 5 shows an overpressure profile of three obstacles against the dimensionless obstacle spacing between the second and third obstacles. The profile is similar to that produced by the positioning of the second obstacle relative to the first obstacle. For 2-flat-bar obstacles, a peak overpressure of 2.2 bar was attained at a separation of 98 obstacle scales (1.25 m separation distance). This distance corresponds to the optimum spacing obtained with two obstacles. In the case of the 4-flat-bar obstacles, a maximum overpressure of 2 bar was realised at the third obstacle spacing of 78 obstacle scales from the second i.e. again at the same relative positioning as the optimum distance of the second obstacle from the first in the two obstacle configuration.

Also shown in Fig. 5 are the flame speed results for the 2 and 4 flat-bar obstacles in the triple obstacle configuration. The flame speeds showed similar turbulence profile and position to peak intensity as the overpressures with maximum flame speed of 569 m/s for the 2-flat-bar and 498 m/s the 4-flat-bar.

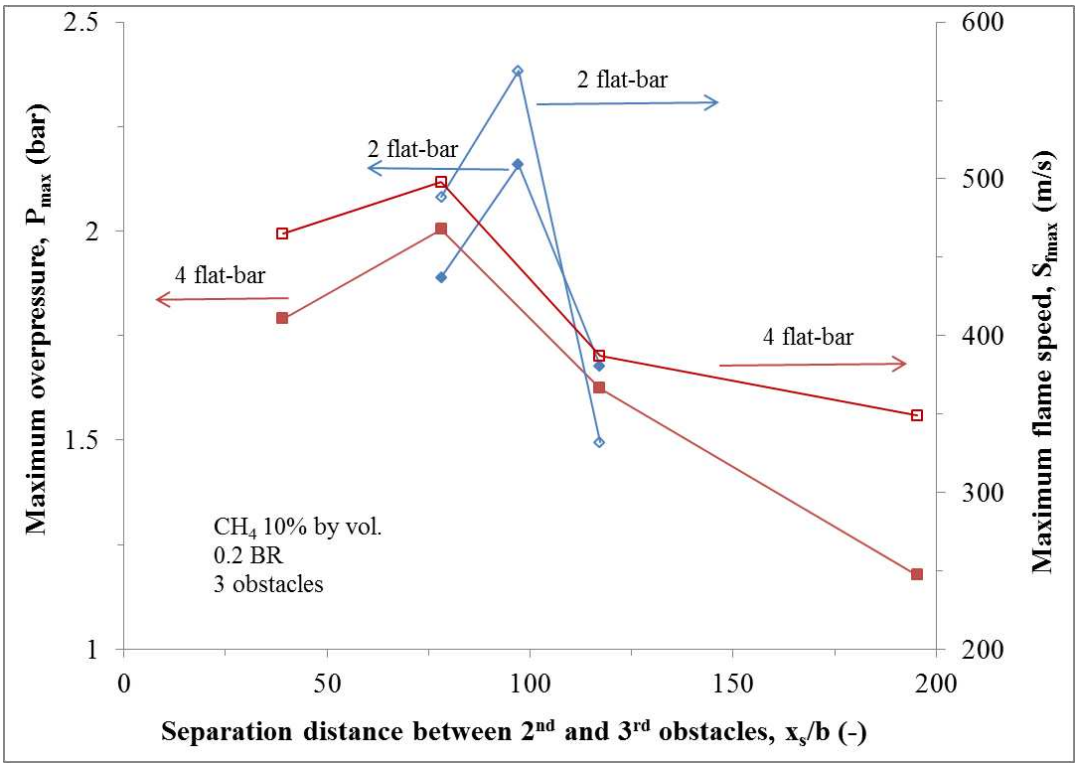

Figure 5: Influence of obstacle separation between 2nd and 3rd obstacles on maximum overpressures and flame speeds.

This work shows that for both obstacle types the optimum spacing between the second and third obstacles corresponded to the same optimum spacing found for the first two obstacles. This suggests that the optimum absolute separation distance does not change with number of obstacles nor with the severity of the explosion, but it does change with the obstacle scale. Therefore this suggests that in multi-obstacle explosions, the spacing between obstacles must be kept away from the worst case explosion severity separation if high overpressures are to be avoided. Wide separation also represents a relatively uncongested scenario and so the

assumption often made that fast explosions require congested volumes might not be the complete picture

3.3 Influence of Number of Obstacles

The influence of number of obstacles as a wider assessment of multi-obstacle congestions typically found in industries have been studied previously by Chapman and Wheeler (1926), Moen *et al.* (1982), Hjertager *et al.* (1988) and Ning *et al.* (2005). All the authors observed that the severity of explosions in terms of overpressure and flame speeds were increased as the number of obstacles increased. However, in all the previous works, only orifice plate obstacles were used to generate turbulence in the system.

Figure 6 shows an overpressure-time profile of 1 to 3 obstacles (2-flat-bar type). The obstacles were spaced at 1.25 m each (98 obstacle scales) which was established in 3.1 to give the worst case obstacle separation distance. Upon ignition, the overpressure-time profile was fairly constant in all the obstacle configurations up to the position of the first obstacle positioned at 6.2D from spark. For all the obstacle tests, a sharp rise in overpressure was noticed downstream of the first obstacle and attained a maximum value of about 0.6 bar. This overpressure value doubled that of the no obstacle test. Subsequently, the overpressure in the first obstacle test attenuated and exited the vent at about 72 ms. Another rise in overpressure behind the second obstacle (14D from spark) was observed for the double and triple obstacle tests and a peak value of close to 1.1 bar was achieved with the former while the latter had about 1.3 bar. However, the time to such maximum overpressures were nearly the same in both scenarios. The maximum overpressures doubled that of the single obstacle test. The overpressure in the double obstacle test later decayed and left the vent at the almost the same time with that of the single obstacle test. As the flame approached the third obstacle (21.6D from spark) in the triple obstacle configuration, an increase in overpressure was measured close to 2.2 bar downstream of the third obstacle. This value was nearly two and four times greater than that of double and single obstacle tests respectively.

The influence of number of obstacles in terms of flame speeds against a dimensionless distance from spark is shown in Fig. 7. The flame speeds in comparison to the patterns shown by pressure-time profile demonstrated similar flame development in all the three tests. Similar maximum flame speed of about 43 m/s upstream and 200 m/s downstream of the first obstacle was achieved in all the test configurations. The double obstacle test attained a maximum value of 386 m/s downstream of the second obstacle. This value nearly doubled that of a single obstacle test (a similar factor obtained with overpressure effect). For the three obstacle configuration, a maximum flame speed value of about one and a half times higher than that of the double obstacle was achieved.

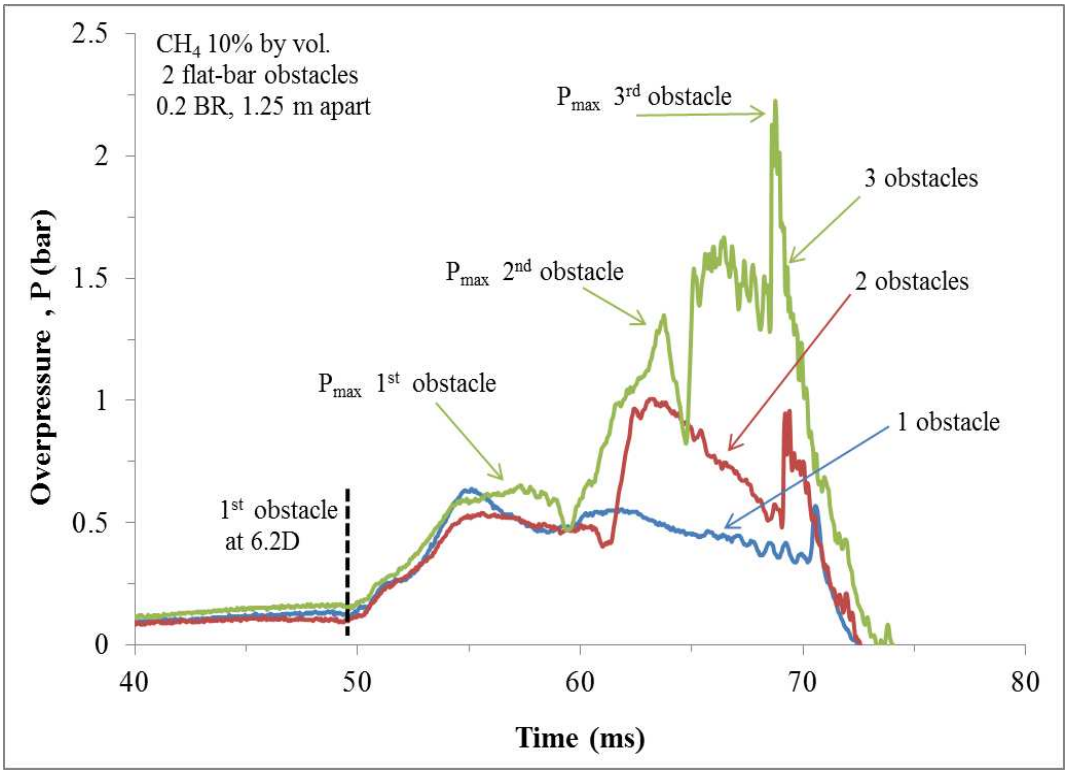

Figure 6: Pressure-time profile for 1, 2 and 3 obstacles spaced at optimum obstacle separation distance.

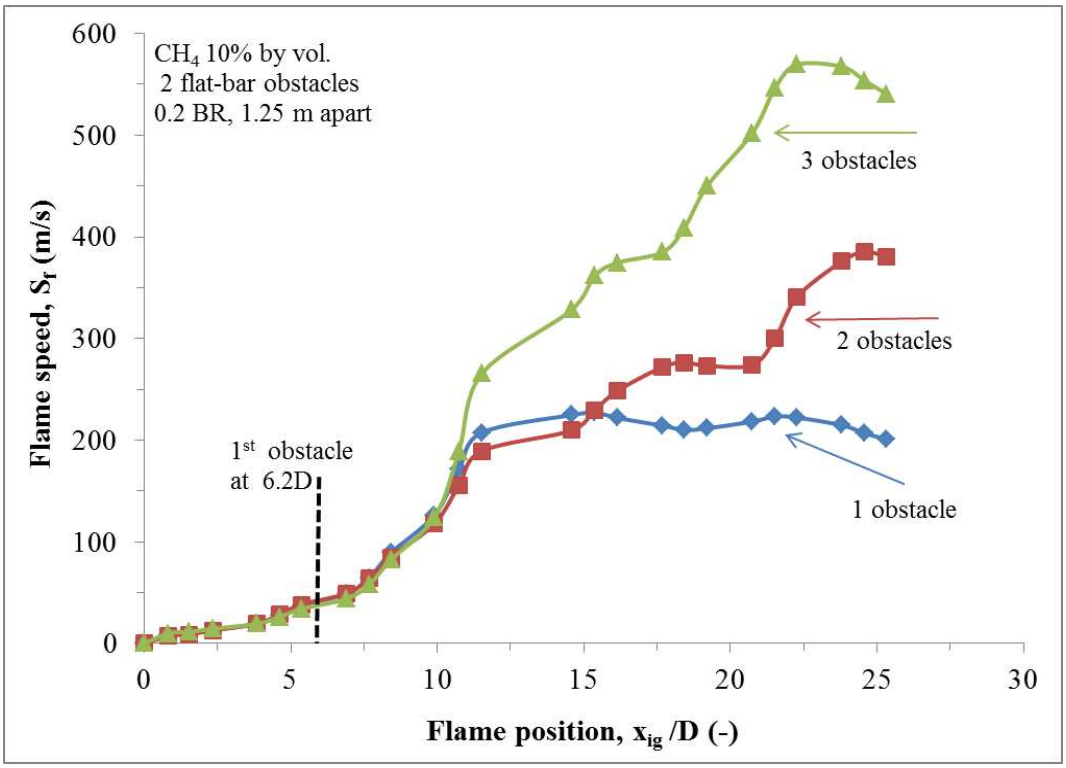

Figure 7: Flame speeds against flame position for 1, 2 and 3 obstacles spaced at optimum obstacle separation distance.

The effect of up to three repeat obstacles on overpressure for 2 and 4 flat-bar obstacles tested in the present research spaced at optimum obstacle separation distance is given in Fig. 8. As shown the overpressure increased significantly with increasing number of obstacles optimally spaced. In all cases the overpressure with the larger scale 2-flat-bar obstacles was 10 to 40% higher than the smaller scale 4-flat-bar ones and this is consistent with the reported effect of scale (ref our groups paper on scale). The biggest effect of scale was observed in the lower over-pressure tests.

In comparison with the literature, Moen *et al.* (1982) studied the influence of number of obstacles on explosion overpressures. The authors performed their tests in a large tube of 2.5 m in diameter and 10 m long corresponding to 50 m^3 by volume. The tube was fully opened at one end and closed at the other and accommodated up to nine regularly spaced orifice plates providing blockage ratios from 0.16 to 0.84. Stoichiometric methane-air mixture ignited at the end of the tube was used to initiate the explosions. For 16% BR obstacles, an overpressure of about 1 bar was achieved with nine plates 1 m apart. This value was 2.2 times lower than that obtained with just three 2-flat-bar obstacles of 0.2 BR in the current work. Also, the authors observed a lower value of overpressure (compared to the present work) of close to 2 bar with three obstacles of 30% blockage. The likely possibility of the lower overpressure in the work of Moen *et al.* (1982) compared to the present one was that the obstacle spacing in the former was not at optimum value as in the case of the present work. However, a general trend of increase in overpressure with number of obstacles was similar in both two tests.

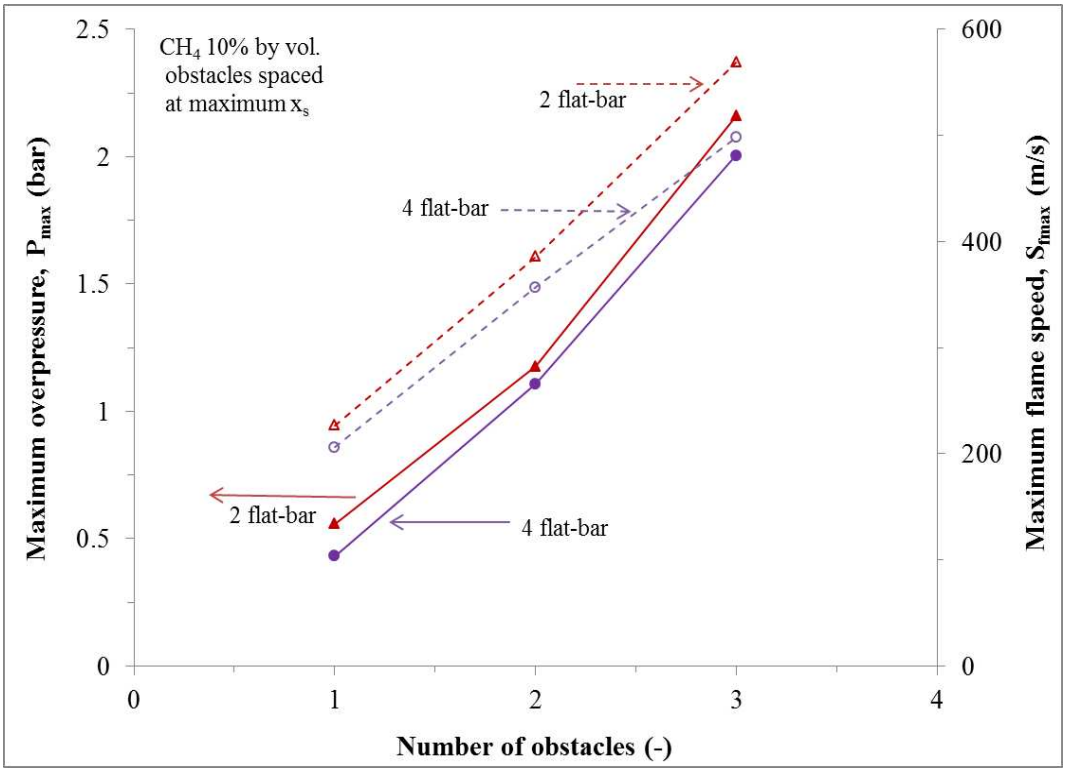

Figure 8: Effect of number of obstacles spaced at optimum position on maximum overpressure for all the obstacles tested in the present research.

Also shown in Fig. 8 is the influence of number of obstacles on maximum flame speed for all the obstacles used in the present research spaced at worst case obstacle separation distance. Patterns similar to overpressures were equally observed with the flame speeds. Also for the

three obstacle configurations, maximum flame speeds of 569 m/s and 498 m/s were obtained for the 2-flat-bar and 4-flat-bar obstacles respectively downstream of the third obstacle.

The highest flame speed from 2-flat-bar obstacles was about 1.4 times higher than that obtained from the pioneer work of Chapman and Wheeler (1926) with up to 20 obstacles of 0.91-0.48 blockage spaced at 5 cm to each other. The explosion geometry used was a brass-tube of 5 cm diameter and 2.4 m long with near stoichiometric methane air mixtures as in the present tests. The maximum flame speed value was achieved at the 12^{th} obstacle, after which an increase in the number of obstacles caused no change. That value was sustained constant throughout the rest of the tube. This behaviour was also observed with overpressure in the work of Moen *et al.* (1982); in their work a reduction in overpressure was observed after the 6^{th} obstacle with 30% obstacle blockage.

4. Conclusions

The profile of effects with separation distance in the present research agreed with the cold flow turbulence profile determined in cold flows by other researchers. However, in the present results the maximum effect in explosions was experienced further downstream than the position of maximum turbulence determined in the cold flow studies. It is suggested that this may be due to the convection of the turbulence profile by the propagating flame.

For the triple obstacle tests, the optimum spacing between the second and third obstacles corresponded to the same optimum spacing found for the first two obstacles (i.e. 80 to 100 obstacle scales) demonstrating that the optimum separation distance does not change with number of obstacles nor the severity of the explosion. This position of maximum flame acceleration was about 3 times further downstream than the position of the maximum turbulence in cold flow turbulence measurements.

Significant increases in explosion overpressures and flame speeds were measure with small increase in number of obstacles spaced at optimum separation distance.

Multi-obstacle studies in the literature have the obstacle spacing (generally) quite close compared to the present work. The results clearly demonstrate that high congestion in a given layout does not necessarily imply higher explosion severity as traditionally assumed. Less congested but optimally separated obstructions can lead to higher overpressures.

In planning the layout of new installations, it is appropriate to identify the relevant worst case obstacle separation in order to avoid it. In assessing the risk to existing installations and taking appropriate mitigation measures it is important to evaluate such risk on the basis of a clear understanding of the effects of separation distance and congestion. The present results would suggest that in many previous studies of repeated obstacles the separation distance investigated might not have included the worst case set up, and therefore existing explosion protection guidelines may not correspond to worst case scenarios.

Acknowledgements

The authors are thankful to the Nigerian Petroleum Technology Development Fund (PTDF) Overseas Scholarship Scheme, for supporting Abdulmajid Na'inna in his PhD studies on the subject.

References

ATEX (1994). ATEX (Explosive Atmosphere) Directives 94/9/EC. European Commission.

Baines, W. D. & Peterson, E. G. (1951). An investigation of flow through screens. *Trans. American Society of Mechanical Engineering,* 73**,** 167.

Beauvais, R., Mayinger, F. & Strube, G. (1993). Severe Accident in a light water reactor: Influence of elevated initial temperature on hydrogen combustion. *ASME/JSME Nuclear Engineering Conference,* 1**,** 425-433.

Boeck, L. R., Hasslberger, J., Ettner, F. & Sattelmayer, T. (Year) Published. Investigation of Peak Pressures during Explosive Combustion of Inhomogeneous Hydrogen-Air Mixtures. Proc. of the Seventh International Seminar on Fire & Explosion Hazards (ISFEH7), 2013 Providence, Rhodes Island. Research Publishing, 959–965.

BS5167-2. (2003). *Measurement of fluid flow by means of pressure differential devices inserted in circular cross-section conduits running full - Part 2: Orifice plates (ISO 5167-2:2003)*. Brussels: European Committee for Standardization.

Chan, C., Moen, I. O. & Lee, J. H. S. (1983). Influence of confinement on flame acceleration due to repeated obstacles. *Combustion and Flame,* 49**,** 27-39.

Chapman, W. R. & Wheeler, R. V. (1926). The propagation of flame in mixtures of methane and air. Part IV. The effect of restrictions in the path of the flame. *Journal of the Chemical Society (Resumed)***,** 2139-2147.

Ciccarelli, G., Fowler, C. J. & Bardon, M. (2005). Effect of obstacle size and spacing on the initial stage of flame acceleration in a rough tube. *Shock Waves,* 14**,** 161-166.

Harrison, A. J. & Eyre, J. A. (1987). The Effect of Obstacle Arrays on the Combustion of Large Premixed Gas/Air Clouds. *Combustion science and technology,* 52**,** 121-137.

Hjertager, B. H., Fuhre, K. & Bjørkhaug, M. (1988). Concentration Effects on Flame Acceleration by Obstacles in Large-Scale Methane-Air and Propane-Air Vented Explosions. *Combustion science and technology,* 62**,** 239-256.

Lee, J. H. S. & Moen, I. O. (1980). The mechans of transition from deflagration to detonation in vapor cloud explosions. *Progress in Energy and Combustion Science,* 6**,** 359-389.

Lindstedt, R. P. & Michels, H. J. (1989). Deflagration to detonation transitions and strong deflagrations in alkane and alkene air mixtures. *Combustion and Flame,* 76**,** 169-181.

Mercx, W. P. M. (1992). Large-scale experimental investigation into vapour cloud explosions: comparison with the small-scale Discoe trials. *Institution of Chemical Engineers,* 70 Part B**,** 197-204.

Moen, I. O., Donato, M., Knystautas, R. & Lee, J. H. (1980). Flame acceleration due to turbulence produced by obstacles. *Combustion and Flame,* 39**,** 21-32.

Moen, I. O., Lee, J. H. S., Hjertager, B. H., Fuhre, K. & Eckhoff, R. K. (1982). Pressure development due to turbulent flame propagation in large-scale methane□air explosions. *Combustion and Flame,* 47**,** 31-52.

Mol'kov, V. V., Agafonov, V. V. & Aleksandrov, S. V. (1997). Deflagration in a vented vessel with internal obstacles. *Combustion, Explosion and Shock Waves,* 33 **,** 418-424.

Na'inna, A. M., Phylaktou, H. N. & Andrews, G. E. (2013a). The acceleration of flames in tube explosions with two obstacles as a function of the obstacle separation distance. *Journal of Loss Prevention in the Process Industries,* 26**,** 1597-1603.

Na'inna, A. M., Phylaktou, H. & Andrews, G. E. (2013b) Published. Acceleration of Flames in Tube Explosions with Two Obstacles as a Function of the Obstacle Separation Distance: The Influence of Mixture Reactivity. Proc. of the Seventh International Seminar on Fire and Explosion Hazards (ISFEH7), 2013 Providence, USA. Research Publishing, 627-636.

Ning, J., Wang, C. & Lu, J. (2005). Influence of obstacles on flame propagation of multi-combustion mixture gas. *Modern Physics Letters B,* 19**,** 1687−1690.

Obara, T., Yajima, S., Yoshihashi, T. & Ohyagi, S. (1996). A high-speed photographic study of the transition from deflagration to detonation wave. *Shock Waves,* 6**,** 205-210.

Pang, L., Zhang, Q., Wang, T., Lin, D. C. & Cheng, L. (2012). Influence of laneway support spacing on methane/air explosion shock wave. *Safety Science,* 50**,** 83-89.

Phylaktou, H.N. & Andrews, G.E. (1991). The acceleration of flame propagation in a tube by an obstacle. *Combustion and Flame,* 85, 363-379.

Porowski, R. & Teodorczyk, A. (2013). Experimental study on DDT for hydrogen–methane–air mixtures in tube with obstacles. *Journal of Loss Prevention in the Process Industries,* 26**,** 374-379.

Rudy, W., Porowski, R. & Teodorczyk, A. (2011). Propagation of hydrogen-air detonation in tube with obstacles. *Journal of Power Technologies,* 91**,** 122-129.

Teodorczyk, A., Drobniak, P. & Dabkowski, A. (2009). Fast turbulent deflagration and DDT of hydrogen–air mixtures in small obstructed channel. *International Journal of Hydrogen Energy,* 34**,** 5887-5893.

Teodorczyk, A., Lee, J. H. S. & Knystautas, R. (1989). Propagation mechanism of quasi-detonations. *Symposium (International) on Combustion,* 22**,** 1723-1731.

Vollmer, K. G., Ettner, F. & Sattelmayer, T. (Year) Published. Deflagration-to-detonation transition in hydrogen-air mixtures with concentration gradients. 23rd International Colloquium on Dynamics of Explosions and Reactive Systems (ICDERS), 24-29 July 2011 Irvine.

Yu, L. X., Sun, W. C. & Wu, C. K. (2002). Flame acceleration and overpressure development in a semiopen tube with repeated obstacles. *Proceedings of the Combustion Institute,* 29**,** 321-327.